

Gravimetric signature of slabs deep thermal structures

Xavier Vergeron^a, Cécilia Cadio^a, Fanny Garel^a
^aGéosciences Montpellier, univ. Montpellier, CNRS, Montpellier, France
Xavier.vergeron@umontpellier.fr

Introduction

- At subduction zones, cold lithospheric plates dive deep into the hotter Earth's mantle.
- Deep Focus Earthquakes are apparently related to their thermal structures.
- Seismic tomography provides a first-order information on slab morphology.
- Geoid and gravity gradients anomalies already evidenced over subduction zones.

Physical concept :

$\Delta T \rightarrow \Delta \rho \rightarrow$ gravity anomaly

Main question :

Can gravity data from the GOCE mission be used to infer slabs' inner thermal structures ?

Focus of this study :

Estimate synthetic gravity data sensitivity to slabs inner thermal structures

Method : from deep (>200 km) slabs thermal structures to synthetic gravity signals

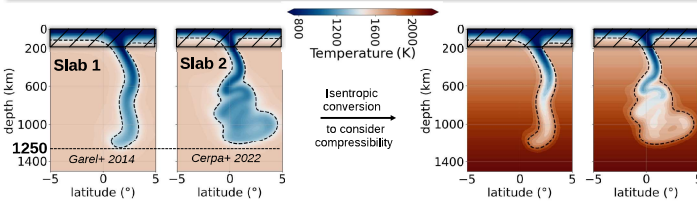


Fig.1 Thermal structure of 2 vertical slabs (~1250 km) from incompressible dynamic models, with the 200 first km removed.

Fig.2 Isentropic thermal structures of slabs 1 and 2

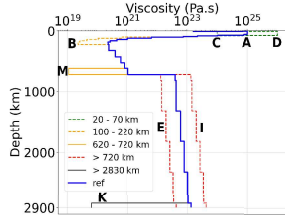


Fig.4. Radial viscosity profiles considered in this study.

Overview of DynG² workflow :
2D vertical grid of density anomalies in cartesian coordinates (input),
series of 2D (global (horizontal) grids of surfacic mass in spherical coordinates, spaced by a vertical step of 5 km,
- converted into spherical harmonics coefficients (SHC).
In parallel, Green's functions calculation, solving mass and momentum conservation equations system for an incompressible Newtonian viscous and spherically symmetric medium assuming a radial viscosity profile,
- Geoid SHC by convolving Green functions and the SHC of the thin layers,
- Geoid SHC adjusted to GOCE mean altitude (255 km)
- Geoid, gravity and gravity gradients grids derived from Geoid adjusted SHC.

Fig.5 schema of a diving slab and mechanically induced surface and CMB deformations, and their individual contribution to the geoid total signal. The slab (positive mass anomaly) contributes positively while surface and CMB deflections respectively contribute negatively at short and long wavelengths.

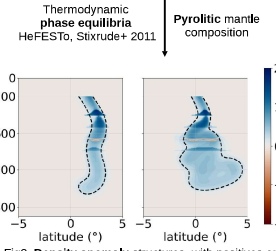


Fig.3. Density anomaly structures, with positives and negative density anomalies due to phase transitions visible into the slab.

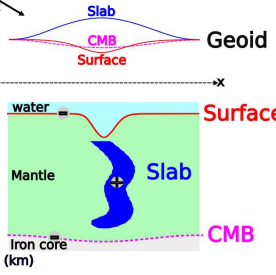
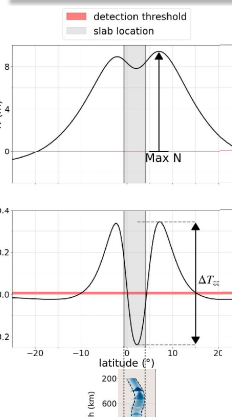


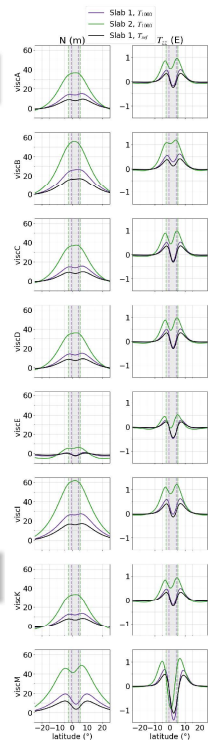
Fig.6. Illustration of modifications applied on deep thermal structures.
-Top: T_{ref} , thermal structure from numerical dynamic subduction model.
-2nd line: F_i , increase or decrease of a factor i (0,5, 0,8, 1,25 or 2) of the thermal spatial gradient inside the slab.
-3rd line: T_c , constant (potential) temperature (800, 1000, 1200 or 1400 K) set to the whole slab.
-4th line : two isothermal regions T_{is} with a shallow colder slab part (T_{is} of 800, 1000 or 1200 K) located above a hotter one (T_{is} of 1000, 1200 or 1400 K) with a transition depth z_t , varying between 300 and 1200 km.
-5th line: two isothermal regions T_{is} with a shallow colder slab part (T_{is} of 800, 1000 or 1200 K) located above a hotter one (T_{is} of 1000, 1200 or 1400 K) with a transition depth z_t , varying between 300 and 1200 km.

Results : synthetic gravity signals



Left : Fig.7 Geoid N and vertical gravity gradient T_{zz} synthetics calculated for the slab 1 with T_{ref} . We focused on the relationship between the geoid maximum amplitude, max N, the central peak-to-peak amplitude of T_{zz} , ΔT_{zz} , and the slab inner thermal structure (SITS). The grey and red areas respectively represent the slab location and GOCE detection threshold.

Right : Fig.8 N and T_{zz} calculated for all viscosity profiles and both morphologies 1 and 2, with T_{200} to avoid any SITS variation effect and focus on viscosity profile and slab's morphology influence on gravity signals. Black line represents the signals calculated for slab 1 with T_{ref} . Slabs 1 and 2 locations are represented by the grey areas and the dashed colored lines (resp. purple and green for slabs 1 and 2). If the slab's morphology and mantle radial viscosity profile control the signals shape at first-order, SITS variations has a significant influence on signals amplitudes.



Slab's temperature vs max N and Delta T_zz

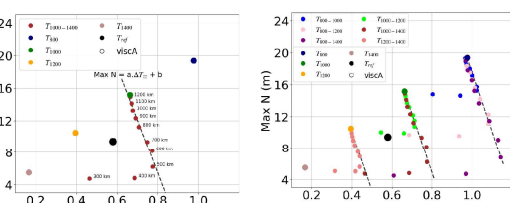
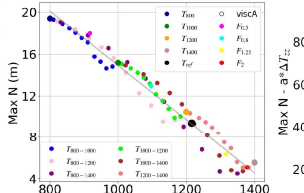


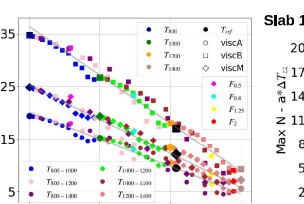
Fig.9 Max N and ΔT_{zz} calculated for viscosity profile A, slab 1 morphology and several SITS. Left : T_{ref} , homogeneous SITS and bi-thermal SITS with $T_1 = 1000$ and $T_2 = 1400$ K. Right : T_{ref} , homogeneous and all bi-thermal SITS. Left subplot illustrates the linear regression feasible on all SITS with the same superficial temperature ($\mu z_2 \geq 500$ km). The slope, a , of this regression remains - the same for all superficial temperatures (cf. right subplot).



Left : Fig.10 Linear relationship between max N and the whole slab's mean temperature.

Right : Fig.11 Linear relationship between max N and ΔT_{zz} , and the slab superficial's (200-500 km) mean temperature.

Both figures are made for slab 1, viscosity profile A and all SITS.



Left side : same as fig.10 but for viscosity profiles A, B and M, and for the slab 1 (top) and 2 (bottom). Right side : same as fig.11 but for viscosity profiles A, B and M, and for the slab 1 (top) and 2 (bottom).

Linear regressions coefficients vary with the slab morphology and the radial viscosity profile of the mantle, but remain feasible for every tested combination of morphology and viscosity profile.

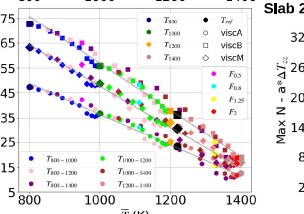
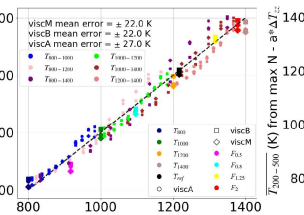


Fig.12 Benchmark of estimated \bar{T} and $T_{200-500}$ for viscosity profiles A, B and M and slab 1 morphology. Mean error < 30 K in each cases.

References :
Cadio, C., et al. "Pacific geoid anomalies revisited in light of thermochemical scaling cones in the lower mantle." Earth and Planetary Science Letters 396L-2 (2011): 123-125.
Cepka, Hestor G., et al. "The effect of a weak asthenospheric layer on surface kinematics, subduction dynamics and slab morphology in the lower mantle." Journal of Geophysical Research: Solid Earth 127A8 (2022): e2022JB024044.



viscM mean error = ± 22.0 K
viscB mean error = ± 22.0 K
viscC mean error = ± 27.0 K
viscD mean error = ± 27.0 K
viscE mean error = ± 27.0 K
viscF mean error = ± 27.0 K
viscG mean error = ± 27.0 K
viscH mean error = ± 27.0 K
viscI mean error = ± 27.0 K
viscJ mean error = ± 27.0 K
viscK mean error = ± 27.0 K
viscL mean error = ± 27.0 K
viscM mean error = ± 23.0 K
viscN mean error = ± 23.0 K
viscO mean error = ± 23.0 K
viscP mean error = ± 23.0 K
viscQ mean error = ± 23.0 K
viscR mean error = ± 23.0 K
viscS mean error = ± 23.0 K
viscT mean error = ± 23.0 K
viscU mean error = ± 23.0 K
viscV mean error = ± 23.0 K
viscW mean error = ± 23.0 K
viscX mean error = ± 23.0 K
viscY mean error = ± 23.0 K
viscZ mean error = ± 23.0 K

viscM mean error = ± 22.0 K
viscB mean error = ± 22.0 K
viscC mean error = ± 27.0 K
viscD mean error = ± 27.0 K
viscE mean error = ± 27.0 K
viscF mean error = ± 27.0 K
viscG mean error = ± 27.0 K
viscH mean error = ± 27.0 K
viscI mean error = ± 27.0 K
viscJ mean error = ± 27.0 K
viscK mean error = ± 27.0 K
viscL mean error = ± 27.0 K
viscM mean error = ± 23.0 K
viscN mean error = ± 23.0 K
viscO mean error = ± 23.0 K
viscP mean error = ± 23.0 K
viscQ mean error = ± 23.0 K
viscR mean error = ± 23.0 K
viscS mean error = ± 23.0 K
viscT mean error = ± 23.0 K
viscU mean error = ± 23.0 K
viscV mean error = ± 23.0 K
viscW mean error = ± 23.0 K
viscX mean error = ± 23.0 K
viscY mean error = ± 23.0 K
viscZ mean error = ± 23.0 K

Take home message

- Max N leads to \bar{T}
- Max N combined with ΔT_{zz} leads to $T_{200-500}$
- Sensitivity of gravity signals to slab's morphology, mantle viscosity profile and SITS
- Gravimetric anomalies amplitude due to SITS modification > GOCE detection threshold

Perspectives

- Synthetic case :
-Develop an inversion strategy based on a priori from seismic tomography
- Natural case :
-Isolate the slab signal from the 200 first km in the total signal
-Apply the inversion strategy to propose a range of possible SITS